Lab on a Chip

Mechanism and Kinetics of Enzymatic Degradation of Polyester Microparticles Using a Shrinking Particle-Shrinking Core Model

Journal:	*Lab on a Chip*
Manuscript ID	LC-ART-07-2023-000581.R1
Article Type:	Paper
Date Submitted by the Author:	01-Sep-2023
Complete List of Authors:	Torabi, Hooman; Cornell University Javi, Farhad; Cornell University, Food Science Deisenroth, Ted; BASF Advanced Formulation Research North America Pho, Toan; BASF Advanced Formulation Research North America Barbright, Victoria; BASF Corporate Abbaspourrad, Alireza; Cornell University, Food Science; Cornell University

Mechanism and Kinetics of Enzymatic Degradation of Polyester Microparticles Using a Shrinking Particle-Shrinking Core Model

Hooman Torabi,[a] Farhad Javi,[a] Ted W Deisenroth,[b] Toan V. Pho,[b] Victoria Barbright,[b] Alireza Abbaspourrad[a]*

[a]Department of Food Science, College of Agriculture & Life Sciences, Cornell University, Stocking Hall, Ithaca, New York, 14853, United States

[b]BASF Corporation, 500 White Plains Road, Tarrytown, New York 10591, United States

* Corresponding Author. Email address: Alireza@cornell.edu

ABSTRACT

Generalized shrinking particle (SPM) and shrinking core (SCM) models were developed to the kinetics of heterogenous enzymatic degradation of polymer microparticles in a continuous microflow system. This enzymatic degradation was performed in a microfluidic device designed to both physically separate and immobilize the microparticles. Then time-resolved measurements were made using image processing of the physical changes of the particles during degradation. The kinetics of enzyme-polymer intermediate formation, enzymatic bond cleavage, and enzyme diffusion through the layer of degraded substrate (SCM only) were mathematically derived to predict the time-resolved degradation of the substrate. The proposed models were tested against the degradation of 15-25 μm particles of polycaprolactone (PCL) and poly (butylene adipate-co-terephthalate) (PBAT) by cutinase enzyme from *Humicola insolens*. Degradation of PCL

microparticles followed the SPM model and its kinetics were found to be zero-order, while the SCM model applied to PBAT microparticles showed first-order kinetics. Further, the degradation of polybutylene succinate (PBS), and poly butylene-sebacate–co–terephthalate (PBSeT) microparticles demonstrated wide applicability of the method. The use of image processing simplifies the required analysis by eliminating the need to remove aliquots or concentrate effluent for additional analytical characterization.

Keywords: Shrinking particle; Shrinking core; Enzymatic degradation; Degradation kinetics; Microfluidics; First-order; Zero-order

INTRODUCTION

Over the past few decades, environmental issues arising from the use and disposal of non-biodegradable polymers have become a worldwide concern for the scientific community, general public, and legislators. To address these concerns, researchers have been working to develop biodegradable polymers and understand the mechanisms involved in their biodegradation. General biodegradation mechanisms that occur through heterogeneous enzymatic degradation involves extracellular enzymes which break polymer chains into shorter pieces which can then be catabolized and become more bioavailable.[1] The first aspect of heterogeneous enzymatic degradation typically consists of four steps: (1) diffusion of the enzyme through the bulk solution to the surface of the substrate; (2) anchoring of the enzyme's active sites to the degradable bonds of the substrate forming a polymer-enzyme active intermediate; (3) catalytic hydrolysis of the bond; and (4) diffusion of degraded materials back to the bulk solution.[2] Each of these steps can affect the overall process where the slowest step is rate determining (RDS). Agitation is used in bulk systems to simplify the process and eliminate steps 1 and 4, because agitation is thought to increase the collision between enzyme molecules and the

substrate. However, the impact of agitation on the kinetics of the degradation is not well understood, and the lack of uniform agitation conditions makes it difficult to compare the results from one study to the next. Furthermore, agitation can adversely affect degradation kinetics by lowering, or completely obscuring, autocatalytic effects.[3] Also, physiological phenomena associated with enzymatic degradation of polymers in nature are known to be slow processes,[4] therefore, static or slow agitation conditions have been suggested to study the enzymatic degradation of such polyesters.[5]

Microfluidic techniques have been used to study polymer degradation on the microscale providing a slow or close-to-static flow of enzyme solution over the substrate.[6–11] The second advantage of microfluidic techniques over degradation in agitated bulk systems is the constant introduction of fresh enzyme to the system removing the effect of enzyme deactivation throughout the process. Enzyme deactivation is an aspect of degradation kinetics which has not been deeply investigated. Previously, we developed a microfluidic device to qualitatively study the enzymatic degradation of a single poly (butylene adipate-co-terephthalate) (PBAT) microparticle.[4] Here we use a similar technique by designing a microfluidic device to study the degradation kinetics of a group of polymer microparticles. Because the associated transport phenomena in a continuous flow system is substantially different, kinetic models developed for bulk systems with agitation cannot be used. Therefore, in addition to developing a continuous flow device to study degradation kinetics, we also developed generalized mathematical models to describe heterogenous enzymatic degradation phenomenon in a continuous system with laminar flow.

Several studies have been focused on the development of a degradation model for water-insoluble polymers. A simple two-step degradation kinetic model similar to the Michaelis-

Menten model has been proposed for enzymatic degradation of polyhydroxy butyrate (PHB) particles,[12] and other polymers.[13,14] This mathematical model assumes a homogenous process even though the polymer substrate is insoluble, and thus it cannot be used to predict what quantity of polymer degrades over time. The equation was then modified to address both the effect of enzyme concentration and the heterogeneity of the substrate.[1] However, because only the initial degradation rate was measured, no relationship was found between the particle's diameter and its rate of degradation.[1]

A different generalized model describing simultaneous autocatalytic and non-autocatalytic reactions[15] was used to study the kinetics of polymer degradation.[16–18] In these studies the autocatalytic and non-autocatalytic processes were not clearly defined and the enzyme is considered solely as the catalyst.[1] Ultimately, this model was found to be more suitable for non-enzymatic, thermal, and mechanical degradation of polymers.

Shrinking Particle (SPM) and Shrinking Core (SCM) models are widely used to describe transport phenomena in solid-fluid chemical reactions,[19–25] including polymer degradation.[26–31] These models by themselves can describe homogenous acid or base hydrolysis of polyethylene terephthalates, but cannot accurately describe the multi-step heterogenous enzymatic degradation of polymers. We postulated that a combined Shrinking Particle (SPM) - Shrinking Core (SCM) model which accounts for each step involved in polymer degradation would more accurately reflect the enzymatic degradation kinetics of polymer microparticles, compared with previously developed kinetic models. Hence, we sought to develop these two models in tandem to describe enzymatic degradation kinetics more accurately.

To achieve our goal, the shape and morphology of the polymer microparticles were monitored during the degradation process using a microfluidic platform with crescent-shape

traps which separated and immobilized a statistical number microparticles. Two key advantages of using a microfluidic platform include: time resolved data; and the ability to measure morphological changes in the substrate using quick, simple, and inexpensive image processing methods.

Microparticles of polycaprolactone (PCL), poly (butylene adipate-co-terephthalate) (PBAT), poly (butylene sebacate-co-terephthalate) (PBSeT), and polybutylene succinate (PBS) were prepared via an oil-in-water solvent removal method. A high-quality statistical sample of particles (10-20), limited by the microscope's view field, was monitored in real-time during degradation by a cutinase enzyme from *Humicola insolens* which efficiently degrades a wide range of polyesters.[32] Image processing was used to assess the morphological changes (size or darkness) and find the RDS. This data was then used to calculate the kinetic parameters. We show that the proposed model for studying polymer microparticle enzymatic degradation on a microfluidic platform is a viable method for assessing enzymatic degradation of water-insoluble polymers.

MATHEMATICAL MODELS

Kinetic model

To develop a mathematical model and measure the kinetics of degradation, the reaction steps must be identified first. Non-catalytic hydrolysis of the polymers studied here was not measurable. Thus, the enzymatic degradation can be described as a two-step process (**Eq. 1**) where a complex between the enzyme molecules and the polymers' surface (*EP*) is formed, and then *EP* cleaves the ester bonds on the surface producing degraded materials (**Eq. 2**). This two-step process is analogous to previous studies.[12,14]

$$\varepsilon E(aq) + P(s) \overset{K}{\rightleftharpoons} EP \quad \textbf{(1)}$$

$$EP \overset{k}{\rightarrow} D \quad \textbf{(2)}$$

Where E is the enzyme present in the solution with the concentration of [E], P is the polymer, D is the degraded material, K is the equilibrium constant for EP and is equal to $\frac{k_f}{k_r}$, k is the catalytic rate constant of D formation and ε is the stoichiometric coefficient.

A general Shrinking Particle Model (SPM) and a Shrinking Core Model (SCM) are proposed (**Fig. 1**) for heterogenous enzymatic degradation of polymer microparticles. The kinetics of each step is mathematically derived assuming they are the rate determining step (RDS). We show the derivation of the governing equation of degradation kinetics if more than one step significantly contributes to the kinetics of degradation.

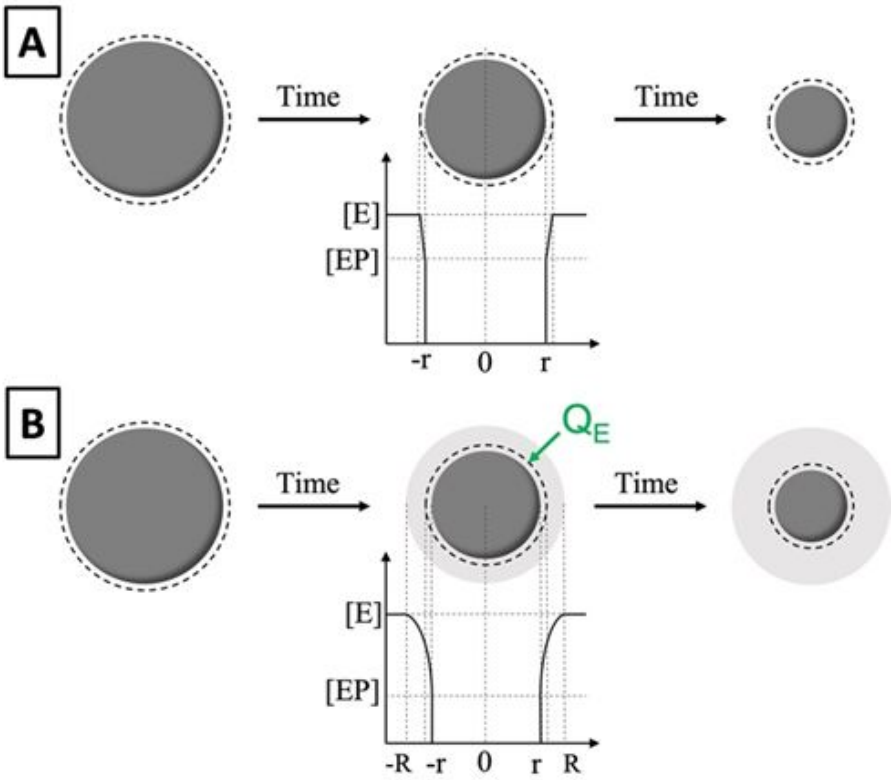

Figure 1: A) Shrinking Particle Model Scheme; A monolayer of intermediate EP (dashed line) is formed on the surface of the particle (solid circle). This layer then transforms to degraded materials. **B)** Shrinking Core Model. A layer of degraded material (light gray) is formed around the unreacted core (dark gray). The total size of the particle remains unchanged while the core continues to shrink as degradation continues, similar to SPM model. Q_E is the flux of enzyme diffusion through the degraded layer.

Shrinking Particle Model (SPM)

During degradation, the polymer segments in contact with enzyme molecules break into increasingly smaller pieces which eventually degrade to hydrophilic oligomers and monomers. In the SPM model, particles continue to shrink as the enzymatic degradation progresses, resulting in a constant reduction of the particle size until full degradation is achieved (**Fig. 1A**). This model is similar to the surface erosion model, where the high crystallinity and hydrophobicity limits the water and enzyme's ability to penetrate through to the core of the particle such that degradation occurs from the surface progressively toward the core.[33] In contrast to the surface erosion model, the SPM model suggests that this phenomenon may arise from the increased solubility of the degraded materials into the surrounding aqueous media leaving the unreacted core of the particle exposed to its surrounding.

From a mechanistic point of view, enzyme molecules form a monolayer on the substrate's surface producing intermediate *EP* (**Eq. 1**). If this step is slower than the polymer's conversion to degraded materials, it is the RDS; we will refer to this as the *EP control* mechanism. Assuming steady-state conditions for enzyme-substrate interaction,[34] all the *EP* formed (N_{EP}) is instantly converted to the degraded material and its net concentration is equal to zero at any given time. Thus, the moles of the polymer consumed is equal to that of consumed *E* and the overall reaction scheme transforms to the following:

$$\varepsilon E(aq) + P(s) \overset{k_f}{\rightarrow} D \qquad \textbf{(3)}$$

$$-\varepsilon \mathrm{r_P} = -\mathrm{r_E} \text{ where } -\varepsilon \frac{d}{dt} N_P = -\frac{d}{dt} N_E \qquad \textbf{(4)}$$

Where r_p and r_E are the rate of consumption of the polymer and enzyme, respectively. Assuming equation **(4)** represents an elementary reaction, the rate of consumption of *E* could be written as the following:

$$-\varepsilon\frac{1}{A_P}\frac{dN_P}{dt} = -\frac{1}{A_P}\frac{dN_E}{dt} = k_f[E] \quad \textbf{(5)}$$

Where A_p is the surface area of the particle and N_p and N_E represent the amount of polymer and enzyme, respectively. Since the reaction takes place on the surface, we write its kinetics according to the surface A_P:

$$-\frac{\varepsilon}{A_P}\frac{d}{dt}N_P = -\frac{\varepsilon}{4\pi r^2}\frac{d}{dt}N_P = -\frac{\varepsilon}{4\pi r^2}4\rho\pi r^2\frac{d}{dt}r = -\varepsilon\rho\frac{d}{dt}r \quad \textbf{(6)}$$

Where *r* is the radius of the particle at any given time t, and ρ is the density of the polymer. Combining equations (**5**) and (**6**), the degradation kinetics can be expressed as:

$$-\varepsilon\rho\frac{d}{dt}r = k_f[E] \quad \textbf{(7)}$$

$$-\int_R^r dr = \frac{k_f[E]}{\varepsilon\rho}\int_0^t dt \quad \textbf{(8)}$$

Solving equation **(8)** and rearranging for time provides:

$$t_{EP} = \tau_{EP}\left[1-\left(\frac{r}{R}\right)\right] \text{ where } \tau_{EP} = \frac{\varepsilon\rho R}{k_f[E]} \quad \textbf{(9)}$$

In equation **(9)**, R is the initial radius of the particle and τ is the time required for the full degradation (characteristic time). The EP subscript denotes the characteristic time associated with the *EP control* mechanism. The direct relationship between τ and R in the degradation of a substrate has been previously observed in other reaction kinetics.[21,35]

If equation **(2)** is the RDS, the formation of the *EP* layer is faster than its consumption;[34] the amount of degraded polymer is equal to that of the *EP* converted to *D*. In other words, the rate of bond cleavage in the polymer backbone dominates the kinetics of degradation. We will refer to this as the *reaction (RXN) control* mechanism. Subsequently:

$$-r_P = -r_{EP} \text{ where } -\frac{d}{dt}N_{EP} = \frac{d}{dt}N_D \quad \textbf{(10)}$$

$$\frac{d}{dt}N_D = k\,[EP] \quad \textbf{(11)}$$

Considering the equilibrium in equation **(1)**:

$$\frac{d}{dt}N_D = k\,K[E]^{\varepsilon} \quad \textbf{(12)}$$

According to the quasi steady-state approximation of enzymatic reactions,[34] the concentration of *EP* is always constant at any given time, however, N_{EP} changes as the A_P shrinks, consequently:

$$N_{EP} = A_P\emptyset \quad \textbf{(13)}$$

$$-\frac{d}{dt}N_{EP} = -8\emptyset\pi r\frac{dr}{dt} \quad \textbf{(14)}$$

Where $\emptyset$ is the enzyme loading per unit of the polymer surface (mole/area) and is a function of [E]. Previous studies reported that the immobilization of enzyme onto the polymer surface follows Langmuir isotherm kinetics,[36] thus:

$$N_{EP} = A_P\emptyset_{max}\frac{K[E]}{1 + K[E]} \quad \textbf{(15)}$$

where $\emptyset_{max}$ is the maximum enzyme loading onto the surface. Combining equations (**12**), (**14**), and (**15**) the kinetics of *EP* consumption can therefore be expressed as follows:

$$-8\pi\emptyset_{max}\frac{K[E]}{1 + K[E]}\,r\frac{dr}{dt} = kK[E]^{\varepsilon} \quad \textbf{(16)}$$

$$-\int_R^r r\,dr = \frac{k[E]^{\varepsilon-1}(1+K[E])}{8\pi\emptyset_{max}}\int_0^t dt \quad \textbf{(17)}$$

Previous measurements of K [1] demonstrated that K[E]<<1, and consequently 1+ K[E] is approximately 1. By solving equation **(17)** and rearranging we get an expression for the time and conversion (r/R):

$$t = \tau\left[1-\left(\frac{r}{R}\right)^2\right] \text{ where } \tau = \frac{A_0\emptyset_{max}}{k[E]^n} \quad \textbf{(18)}$$

In equation **(18)**, A_0 is the initial surface area of the particle and $n = \varepsilon - 1$. The direct relation of τ_{RXN} and A_0 in equation **(18)** is analogous to a model reported previously.[31] The measurement of enzyme loading in previous studies was reported as 0.25 ng cm^{-2}.[37] To simplify the calculations, an apparent rate coefficient *k'* is assumed and equation **(18)** transforms to the following:

$$k' = \frac{k}{\emptyset_{max}} \quad \textbf{(19)}$$

$$t_{RXN} = \tau_{RXN}\left[1-\left(\frac{r}{R}\right)^2\right] \text{ where } \tau_{RXN} = \frac{A_0}{k'[E]^n} \quad \textbf{(20)}$$

Shrinking Core Model (SCM)

The shrinking core model (SCM) applies to particles where microparticle size is not affected by the degradation reaction; the particles maintain their initial shape and size during the degradation. This mode of degradation is similar to bulk degradation[33] also known as the progressive conversion model, with a substantial difference. In the bulk degradation mechanism, the enzyme molecules penetrate through the surface of the particle to the core and no gradient of enzyme concentration within the particle is assumed.[33] Because of these assumptions, the bulk degradation model only applies to highly porous particles. The shrinking core model addresses this issue assuming an unreacted core above which a stable layer of degraded materials, *D,* is

formed, which we refer to as the ash layer. No enzyme penetration through the surface of the unreacted core is assumed, however enzyme does penetrate the ash layer, the thickness of which increases over time **(Fig. 1B)**.

The SCM mechanism for degradation remains similar to the SPM such that equations **(1)** and **(2)** apply to the SCM, therefore, equations (**9**) and (**20**) apply to this model as well. However, since the enzyme molecules must diffuse through the ash layer to reach to the core's surface, a gradient in enzyme concentration inside the ash layer must be considered **(Fig. 1B)**. Assuming the steady state condition, the rate of change of [E] (dN_E) is equal to its rate of diffusion through the ash layer. A previously reported model for gas-solid reactions describes the diffusion of reactants through the ash layer.[38] This model is also applicable for liquid-solid reactions if the velocity ratio (liquid flow rate over solid's shrinkage rate) is larger than unity. In experiments performed in microfluidic devices, the flow velocity and the particles' shrinkage rate were calculated to be 0.1 m h^{-1} and maximum 25 μm h^{-1}, respectively. Thus, the velocity ratio is several orders of magnitude larger than unity. As a result, a previously reported formulae for gas-solid reactions can also be used here.[35] Assuming the diffusion follows Fick's law:

$$-\varepsilon\frac{d}{dt}N_P = -\frac{d}{dt}N_E = 4\pi r^2 Q_E \quad \textbf{(21)}$$

$$Q_E = \mathcal{D}\frac{d[E]}{dr} \quad \textbf{(22)}$$

In equation (**22**), $\mathcal{D}$ is the diffusion coefficient of enzyme molecules through the ash layer and Q_E is the flux of diffusion. By combining equations (**21**) and **(22)**:

$$-\frac{d}{dt}N_E = 4\pi r^2 \mathcal{D}\frac{d[E]}{dr} \quad \textbf{(23)}$$

Integration of equation (**23**) across the ash layer shows that at any given time, dN_E is constant and proportional to the diffusion coefficient $\mathcal{D}$.

$$-\frac{d}{dt}N_E\left(\frac{1}{r}-\frac{1}{R}\right)=4\pi\mathcal{D}[E] \quad \textbf{(24)}$$

Combining equations (**6**), (**21**), (**23**) and (**24**) will result in the following:

$$-\varepsilon\rho\int_R^r\left(\frac{1}{r}-\frac{1}{R}\right)r^2dr=\ \mathcal{D}[E]\int_0^t dt \quad \textbf{(25)}$$

Solving equation (**25**) and rearranging provides an expression for the kinetics of SCM degradation if diffusion is the RDS:

$$t_{\mathcal{D}}=\tau_{\mathcal{D}}\left[1-3\left(\frac{r}{R}\right)^2+2\left(\frac{r}{R}\right)^3\right]\ \text{where}\ \tau_{\mathcal{D}}=\frac{\varepsilon\rho R^2}{6\mathcal{D}[E]} \quad \textbf{(26)}$$

To elucidate the degradation kinetics, the characteristic time (τ) and its relation to the particle size (R) must first be found to identify the RDS. The experimental time-conversion data (r/R vs. t) for particles with different radii should be fitted with possible RDS models at a certain enzyme concentration. Note that the conversion is defined as the radius of the particle (SPM), or unreacted core (SCM) normalized to their initial value (r/R).

Once the RDS is found, the kinetic parameters K, k', n, and $\mathcal{D}$ can be calculated by finding the relation between τ and [E] (**Eqs. 9, 20, and 26**). In this regard, degradation of particles should be performed using enzyme at different concentrations and the characteristic time and enzyme concentration data (τ vs. [E]) fitted to the associated RDS model. Notably, in the SCM mechanism, if diffusion affects the degradation kinetics alongside another RDS, then the time-conversion relationship can be assumed as the combination of diffusion and the other effective step. A schematic of the experiments performed in microfluidic system to show the

degradation kinetics by tracking the real-time conversion of microparticles (r/R) is illustrated in **Fig. 2**. The methods used for loading microchannels and running the experiments are briefly discussed in supporting information per our previous study.[4] Additionally, the supporting information contains a summary of SPM-SCM model, associated RDSs, and typical conversion-time graphs are provided in **Table S1** and **Fig. S1**, respectively.

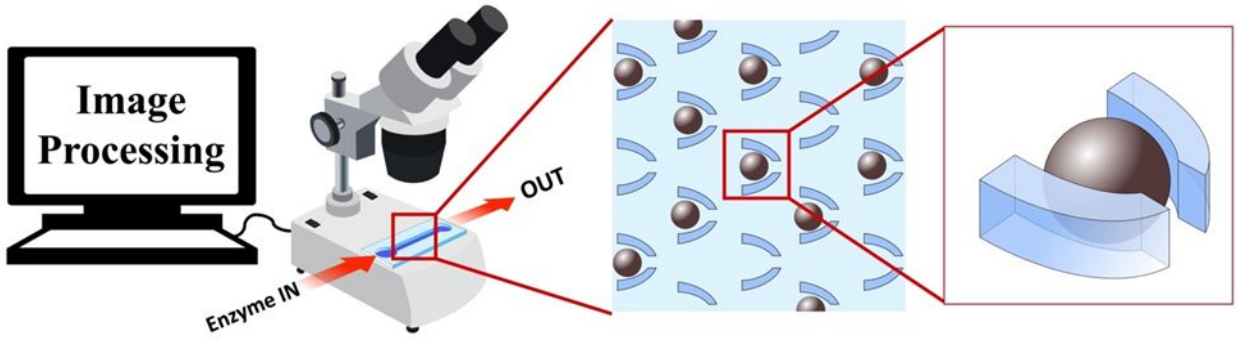

Figure 2. Schematics of experimental setup and the structure of microfluidic device. Dark spheres represent polymer microparticles.

RESULTS AND DISCUSSIONS

Shrinking particles

Enzymatic degradation of PCL particles with ~15 µm and ~30 µm in radius was performed using enzyme at 150 LU g^{-1} with a flow rate of 10 µL h^{-1}. These particles experience a constant reduction in size, following the shrinking particle pattern **(Fig. 3A and B)**. Particle conversion (r/R) was calculated over time by measuring the change in the particles' radius using image processing method.

Fitting r/R versus t with intermediate formation (*EP control)* mechanism predicted the τ at ~140 min for 15 µm particles and ~470 min for 30 µm particles (**Fig. S5** and **Table S3**). These values were higher than the experimental time observations, therefore the *EP control* cannot be

the RDS (**Fig. 3A and B**). The bond cleavage (*RXN control*) mechanism predicts τ equal to be 91 mins for ~15 µm particles and 275 mins for ~30 µm particles (**Fig. 3C** and **D**). In our experimental observations particles were found to be completely degraded within similar time frames, thus indicating that this RDS model was a good fit **(Fig. 3** and **Movie S1)**. Further, if the

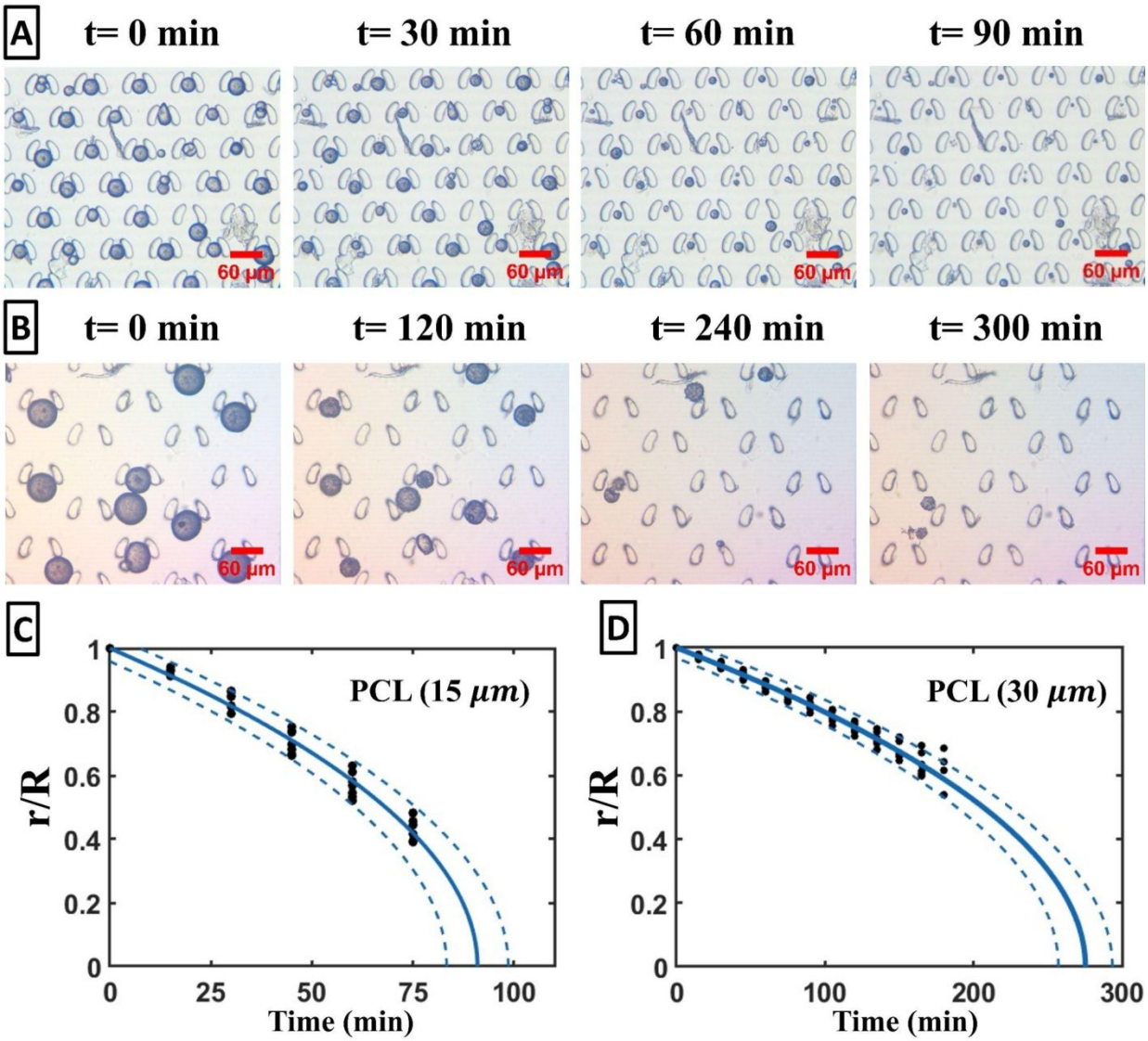

Figure 3: Time lapse of enzymatic degradation of PCL particles with **A**) ~15 µm and **B**) ~30 µm in radius using 150 LU g^{-1} enzyme solution (scale bar = 60 µm). Conversion-time data of enzymatic degradation of PCL micro particles (black dots) with **C**) ~15 µm and **D**) ~30 µm and fitted curves of *RXN control* mechanism (blue line). Dashed lines indicate 95% confidence bands.

RXN control mechanism is the RDS, because τ is a function of A_0, the normalized characteristic time (τ/A_0) should remain constant for particles with a difference in radius at any specific enzyme concentration [E]. Our calculations indicate that the value of (τ/A_0) for ~30 μm particles and ~15 μm particles is not significantly different ($p < 0.05$) (**Table 1**). The close match of the experimentally observed and the calculated (τ/A_0) indicates that enzymatic particle degradation is governed by *RXN control* mechanism.

Using the identified RDS, the rate constant *k'* and *n* is calculated by performing similar experiments on ~15 μm particles using the enzyme at 1500 and 150 LU g^{-1} concentrations (**Fig. S6**). The degradation kinetics of PCL were found to be independent of enzyme concentration from 15 kLU g^{-1} to 150 LU g^{-1}, indicating that the enzymatic degradation of PCL particles is a zero-order reaction governed by the *RXN control* mechanism (**Table 1**). The rate of degradation of PCL particles equation thus transforms to $(\frac{r}{R})^2 = 1 - \frac{k'}{A_0}t$, where *k'* = 34.6 ± 2.5 μm^2 min^{-1} using **Eq. 20**.

Unlike our findings, a previously developed model for enzymatic degradation of PCL and other polyester microparticles suggests a linear relationship between conversion and time (r/R vs. t), even though their experimental results did not comply with that model especially, at higher conversion rates [(r/R) < 0.4].[1] This is a clear indication of the advantages of our SPM-SCM model over inaccuracies in the previously reported model as it accurately predicts the mechanism of degradation, characteristic time, and conversion rate at any given time.

Core-shrinking particles

PBAT is an aromatic aliphatic polyester containing hard and soft segments. These particles, upon enzymatic degradation, do not experience shrinkage, rather, their appearance

289 transforms from opaque to transparent.[4] The size of the unreacted core shrinks as the degradation
290 proceeds which makes this polymer a suitable candidate on which to apply the shrinking-core
291 model.

Table 1: Detailed results for enzymatic degradation of PCL microparticles assuming ***RXN control*** degradation mechanism

[E]	15 kLU g^{-1}	1.5 kLU g^{-1}	150 LU g^{-1}	150 LU g^{-1}
Radius (μm)	15.9 ± 1.1	15.6 ± 0.6	16.2 ± 1.2	28.8 ± 1.0
τ (min)*	95.3 ± 1.7	92.5 ± 1.3	90.9 ± 1.1	275.2 ± 2.6
$\frac{\tau}{A_0} \times 10^2$ (min μm^{-2})	3.06 ± 0.37[a]	3.04 ± 0.32[a]	2.78 ± 0.38[a]	2.65 ± 0.2[a]
k' (μm min^{-1})	33.0 ± 4.0[b]	33.1 ± 3.5[b]	36.3 ± 4.9[b]	37.8 ± 2.2[b]

* Predicted by the model assuming *RXN control* mechanism as the RDS.
Similar letters in each row indicate no significant statistical difference by one-way ANOVA Tukey's test ($p<0.05$). Values were given as mean±SD.

292

293 To find the RDS, PBAT particles with ~20 μm radii were subjected to degradation using
294 15 kLU g^{-1} enzyme solution **(Fig. 4A,** and **Movie S2)**. The appearance of the particles as they
295 shifted from opaque particles to transparent particles was monitored over time. To quantify the
296 changes, the average gray value of the particle, at any given time, was measured by image
297 processing tools and normalized to its maximum (background) and the minimum (darkest). Thus,
298 the darkness was calculated as following:

299 $$relative\ darkness = 1 - \frac{particles\ gray\ value - minimum\ particle\ gray\ value}{background\ gray\ value - minimum\ particle\ gray\ value} \quad (28)$$

300 Once the particles' darkness reaches a minimum (maximum transparency), the
301 degradation was considered completed and τ was found to be ~68 h. We observed that the
302 particles get slightly darker (~10%) at the initial stages of degradation **(Fig. 4C)**. We attribute
303 this to the degradation of the amorphous regions on the surface of the particle, which led to an
304 initial increase in the ratio of crystalline regions to amorphous regions of the substrate which

caused the particles to diffract light and appear darker.[5] Nevertheless, monitoring the change in particle darkness fails to provide accurate time-resolved information for the shrinkage of the core (r/R vs. t).

According to SCM model, water (and enzyme) molecules cannot penetrate through the unreacted core, and the reactions take place solely on its surface . To evaluate this assumption, PBAT microparticles were immobilized in the microfluidic channel and treated with a buffer solution containing fluorescein dye (no enzyme added). No change in the fluorescence properties of the particles was observed after 48 h, confirming the impermeability of the particles (**Fig. S7**).

The ash layer, however, is assumed to be permeable to water and other solutes in the solution. Thus, fluorescence imaging can be used to distinguish the unreacted core from the ash layer. The difference in fluorescence between the ash layer and unreacted core allowed for a more accurate measurement of the radius of the ash layer compared to the unreacted core and confirmed the shrinking core degradation mechanism at the initial stage of degradation (r/R>0.6) (**Fig. S8**). After that, the difference in contrast between the ash and unreacted core decreases to the point at which the radius of unreacted core becomes immeasurable.

Plotting conversion (r/R) versus time as extrapolated from the results of fluorescent imaging with the proposed RDS models suggests that the enzymatic degradation of PBAT particles is governed by the *RXN control* mechanism (**Table S4 and Fig. S9**). This mechanism most accurately predicts the characteristic time, τ, which for core-shrinking particles is equal to the time required for particles' darkness to reach a minimum **(Fig. 4C and Table S4)**. In order to confirm this, τ was calculated for ~15 μm particles under similar test conditions and was found to be ~33 h **(Fig. 4B and C)**. Because the normalized characteristic times ($\frac{\tau}{A_0}$) for ~20 μm

particles and ~15 µm particles were not significantly different ($p < 0.05$), the *RXN control* mechanism is found as the RDS (**Table 2**).

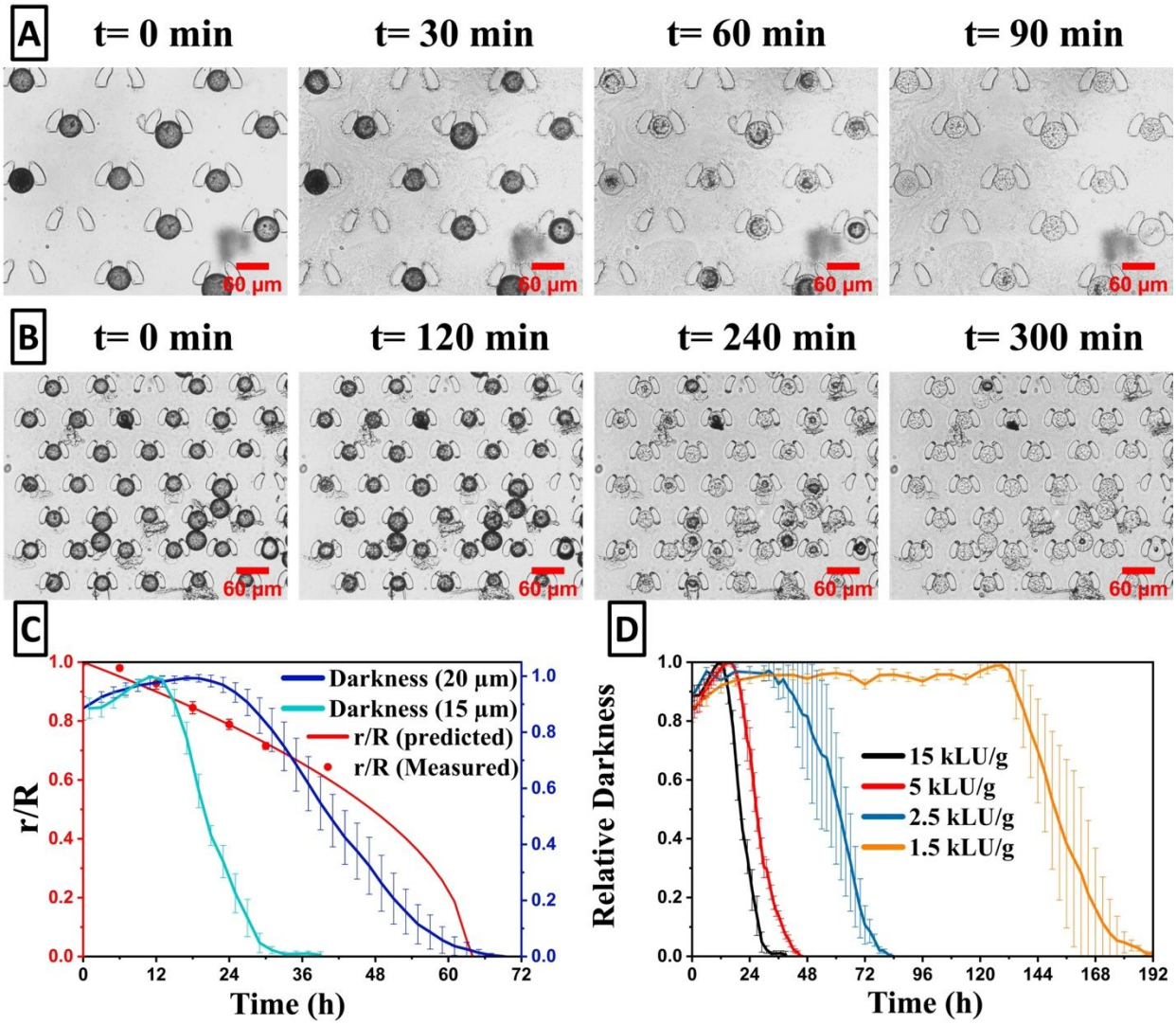

Figure 4: Time lapse of enzymatic degradation of PBAT microparticles with **A)** ~20 µm and **B)** ~15 µm in radius using enzyme at 15 kLU g^{-1}. Scale bar is 60 µm. **C)** Comparison of relative darkness and conversion rate (r/R) for PBAT particles. r/R was measured for particles with ~20 µm in radius from fluorescent images (red dots). Predicted curve (red line) denotes the regression of measured r/R assuming *RXN control* mechanism as the RDS. **D)** change in the relative darkness of PBAT particles with ~15 µm in radius using enzyme at different

The degradation of 15 µm particles was further investigated using different concentrations of enzyme to calculate *k'* and *n* (**Table 2,** timelapse of experiment in **Fig. S10**). The change in particle darkness over time was monitored to measure the τ **(Fig. 4D)**. Then by fitting $(\frac{\tau}{A_0} vs.\ [E])$ using equation **(20),** we found that the overall degradation rate of PBAT that was first-order $(n = 0.98 \pm 0.04)$ **(Fig. 5)**. The overall equation for the rate of degradation transforms to $\left(\frac{r}{R}\right)^2 = 1 - \frac{k'}{A_0}[E]t$ were $k' = (1.31 \pm 0.02) \times 10^{-2}\left[\frac{g.\ \mu m^2}{kLU.\ h}\right]$.

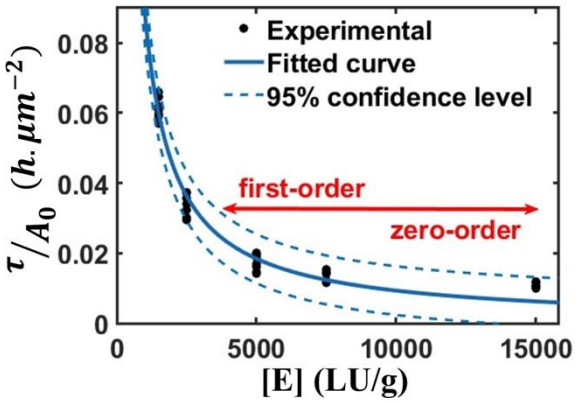

Figure 5: Calculated τ/A_0 vs. [E] for PBAT microparticles with ~15 µm in radius and fitted curve assuming $\frac{\tau}{A_0} = \frac{1}{k'[E]^n}$

Table 2: Detailed results for enzymatic degradation of PBAT microparticles

[E]	15 kLU g^{-1}	15 kLU g^{-1}	7.5 kLU g^{-1}	5 kLU g^{-1}	2.5 kLU g^{-1}	1.5 kLU g^{-1}
Radius (µm)	22.1±1.5	15.6 ± 0.7	16.5 ± 0.8	14.5 ± 1.0	14.0 ± .9	15.4±0.4
τ (h)	64.7±1.9	33.3 ± 1.9	45.0 ± 2.7	45.7 ± 0.4	83.4 ± 3.9	181.7 ± 8.6
$\frac{\tau}{A_0} \times 10^2$ (h μm^{-2})	1.06 ±0.14[a]	1.08 ±0.07[a]	1.32 ±0.15[b]	1.75 ±0.23[c]	3.37 ±0.32[d]	6.13 ± 0.3[e]

Different letters in each row indicate significant statistical difference by one-way ANOVA Tukey's test ($p<0.05$). Values were given as mean ± SD.

Experimental results indicate that enzyme concentrations above 7.5 kLU g^{-1} only mildly affect τ, therefore, the degradation kinetics are zero-order under such conditions. However, when the enzyme concentration is lower than 7.5 kLU g^{-1} the degradation kinetics become first order **(Fig. 5).** Similarly, the classic Michaelis-Menten model suggests zero-order reaction at high [E] (lower substrate concentration) and first order at low [E] (higher substrate concentration). These findings are consistent with previous reports in which zero-order and first order kinetics were attributed to "enzyme excess" and "surface excess" conditions, respectively.[1]

PBSeT is another aromatic aliphatic co-polymer which contains longer aliphatic soft segments (sebacate) compared to PBAT (adipate). The degradation of PBSeT microparticles with ~15 μm radii exhibited a similar pattern as PBAT particles using 1.5 kLU g^{-1} enzyme solution. The characteristic time was found to be ~95 h, which is almost half the characteristic time calculated for PBAT under these conditions (**Fig. S11 and S13**). Previous reports claimed that the presence of longer aliphatic chains, or a lower content of aromatic segments, contributed to an increase in enzyme activity due to the lower ability of PBSeT to form hard segment microdomains compared with PBAT.[39] Others have reported that the effect of polymer's chemical structure on enzymatic hydrolysis outweighs the effect of the substrate's crystallinity.[1] Our results support the latter hypothesis considering our observation that PBSeT degraded almost twice as fast as PBAT, but PBSeT has higher crystallinity (26%) than PBAT (12%).

To extend this, enzymatic degradation of PBS microparticles was studied. PBS possesses a fully aliphatic backbone with shorter soft segments (succinate) compared to PBAT but with higher crystallinity (43%). PBS particles fully degrade in ~70 h using only 150 LU g^{-1} (**Fig. S12-13**). Comparing the degradation rates and the degree of crystallinity of PBAT, PBSeT, and PBS, we believe that the chemical structure of the substrate has a more profound effect on the kinetics

of degradation, rather than their extent of crystallinity. One should note that PBS microparticles possess macropores and not micropores (**Fig. S2**). The preparation of microparticles from different polymer families using a solvent evaporation method comes with unavoidable difference in micro- and macro- pore formation and their corresponding pore sizes. Despite this drawback, this method enabled us to qualitatively compare the effect of the degree of crystallinity versus chemical structure on the degradation rate. Nevertheless, to have a solid conclusion on the effect of substrate's chemical structure and crystallinity on the degradation kinetics, a more systematic and comprehensive study is required, which is outside the scope of this report.

CONCLUSION

Generalized Shrinking Particle (SPM) and Shrinking Core (SCM) models were developed to describe the steps involved in the enzymatic degradation kinetics of polymers with varying chemical compositions and crystallinity. Enzymatic degradation was performed on a microfluidic device to collect time-resolved data regarding the degradation of PCL and PBAT microparticles via image processing methods. PCL particles followed the SPM model, while the degradation PBAT, PBSeT, and PBS microparticles followed the SCM model.

The degradation of PCL microparticles was explained by plotting their time-conversion data, derived from monitoring the change in their size, with all the possible mechanisms of degradation. The bond cleavage (*RXN control*) mechanism accurately predicted the time required for full degradation of PCL with zero-order kinetics.

By monitoring PBAT particles during degradation we observed changes in their darkness and full degradation was determined when the particles were completely transparent. Fluorescent

imaging successfully distinguished the unreacted core of the PBAT microparticles from the ash layer. This enabled measurement of the size of the unreacted core throughout the initial stages of degradation. The RDS for the degradation of PBAT microparticles was found by fitting experimental degradation time from fluorescent imaging to the possible RDS equations proposed for the SCM. Considering the predicted full degradation time, it was found that PBAT degradation is similar to PCL degradation and follows the bond cleavage (*RXN Control*) mechanism with first-order kinetics.

Degradation of PBSeT and PBS microparticles were also briefly studied. No direct correlation between the crystallinity of substrates and degradation kinetics was found and chemical structure seems to dominate these phenomena.

The combination of a microfluidic platform, coupled with the proposed models can be used to shed light on enzymatic degradation mechanisms. We demonstrated the robustness and accuracy of the described model integrated with a microfluidic platform that can be used as a standard method to correlate and elucidate the kinetic parameters of the degradation of water-insoluble polymers.

SUPPORTING INFORMATION

Supporting information is available online and contains additional methods and materials, SEM images, thermal analysis, microfluidic platform fabrication, image processing parameters, supporting data, and Movies S1 and S2.

ACKNOWLEDGEMENTS

We would like to thank the Cornell Center for Materials Research (CCMR) for the use of their facilities. CCMR facilities are supported by the National Science Foundation (United States) under award number DMR- 1719875. We would like to acknowledge the BASF Corporation for their continued support of academic and research pursuits.

CRediT AUTHOR STATEMENT

Hooman Torabi: Conceptualization, Data curation, Formal analysis, Investigation, Methodology, Visualization, Writing - original draft, Writing - review & editing; **Farhard Javi:** Methodology, Visualization; Writing - review & editing; **Ted W Deisenroth:** Conceptualization, Funding acquisition, Project administration, Resources, Writing - review & editing; **Toan Van Pho:** Conceptualization, Writing - review & editing; **Victoria Barbright:** Investigation, Writing - review & editing; **Alireza Abbaspourrad:** Conceptualization, Funding acquisition, Supervision, Project administration, Writing-review & editing;

REFERENCES

1 K. Herzog, R.-J. Müller and W.-D. Deckwer, *Polymer degradation and stability*, 2006, **91**, 2486–2498.
2 M. Rahmouni, F. Chouinard, F. Nekka, V. Lenaerts and J. C. Leroux, *European journal of pharmaceutics and biopharmaceutics*, 2001, **51**, 191–198.
3 L. Liu, S. Li, H. Garreau and M. Vert, *Biomacromolecules*, 2000, **1**, 350–359.
4 S. M. Davachi, A. Mokhtare, H. Torabi, M. Enayati, T. Deisenroth, T. Van Pho, L. Qu, K.-S. Tücking and A. Abbaspourrad, *ACS Omega,* 2023, **8**, 1710–1722
5 S. Li, *Journal of Biomedical Materials Research: An Official Journal of The Society for Biomaterials, The Japanese Society for Biomaterials, and The Australian Society for Biomaterials*, 1999, **48**, 342–353.
6 S. Schusser, M. Krischer, M. Bäcker, A. Poghossian, P. Wagner and M. J. Schöning, *Analytical chemistry*, 2015, **87**, 6607–6613.
7 M. Leinhos, S. Schusser, B. Bachmann, M. Bäcker, A. Poghossian and M. J. Schöning, *physica status solidi (a)*, 2014, **211**, 1346–1351.
8 P. Nghe, P. Tabeling and A. Ajdari, *Journal of Non-Newtonian Fluid Mechanics*, 2010, **165**, 313–322.

9 A. C. R. Grayson, I. S. Choi, B. M. Tyler, P. P. Wang, H. Brem, M. J. Cima and R. Langer, *Nature materials*, 2003, **2**, 767–772.
10 J. Intra, J. M. Glasgow, H. Q. Mai and A. K. Salem, *Journal of Controlled Release*, 2008, **127**, 280–287.
11 B. Wouters, B. W. Pirok, D. Soulis, R. C. G. Perticarini, S. Fokker, R. S. van den Hurk, M. Skolimowski, R. A. Peters and P. J. Schoenmakers, *Analytica chimica acta*, 2019, **1053**, 62–69.
12 M. Scandola, M. L. Focarete and G. Frisoni, *Macromolecules*, 1998, **31**, 3846–3851.
13 P. Polyák, E. Dohovits, G. N. Nagy, B. G. Vértessy, G. Vörös and B. Pukánszky, *International journal of biological macromolecules*, 2018, **112**, 156–162.
14 Å. M. Ronkvist, W. Xie, W. Lu and R. A. Gross, *Macromolecules*, 2009, **42**, 5128–5138.
15 F. Mata-Perez and J. F. Perez-Benito, *Journal of Chemical Education*, 1987, **64**, 925.
16 Y. Xu, S. Sen, Q. Wu, X. Zhong, R. H. Ewoldt and S. C. Zimmerman, *Chemical science*, 2020, **11**, 3326–3331.
17 K. Osada, R. Akahori, Y. Suzuki and A. Matsumoto, *Polymer Degradation and Stability*, 2022, 110127.
18 K. A. Miller, E. G. Morado, S. R. Samanta, B. A. Walker, A. Z. Nelson, S. Sen, D. T. Tran, D. J. Whitaker, R. H. Ewoldt and P. V. Braun, *Journal of the American Chemical Society*, 2019, **141**, 2838–2842.
19 E. Ranzi, M. Corbetta, F. Manenti and S. Pierucci, *Chemical Engineering Science*, 2014, **110**, 2–12.
20 T. Salmi, H. Grénman, J. Wärnå and D. Y. Murzin, *Chemical Engineering and Processing: Process Intensification*, 2011, **50**, 1076–1084.
21 S. Homma, S. Ogata, J. Koga and S. Matsumoto, *Chemical Engineering Science*, 2005, **60**, 4971–4980.
22 H. Gou, G. Zhang, X. Hu and K. Chou, *Transactions of Nonferrous Metals Society of China*, 2017, **27**, 1856–1861.
23 D. Li, Y. Wang and Z. Li, *Catalysts*, 2022, **12**, 1661.
24 D. da Rocha, E. Paetzold and N. Kanswohl, *Chemical Engineering and Processing: Process Intensification*, 2013, **70**, 294–300.
25 S. M. Hashemi, M. H. Sedghkerdar and N. Mahinpey, *The Canadian Journal of Chemical Engineering*, 2022, **100**, 2140–2171.
26 H. Abedsoltan and M. R. Coleman, *Journal of Applied Polymer Science*, 2022, **139**, e52451.
27 H. Abedsoltan, I. S. Omodolor, A. C. Alba-Rubio and M. R. Coleman, *Polymer*, 2021, **222**, 123620.
28 L. Biermann, D. Quast, E. Brepohl, C. Eichert and S. Scholl, *Chemical Engineering & Technology*, 2021, **44**, 2300–2308.
29 R. López-Fonseca, J. R. González-Velasco and J. I. Gutiérrez-Ortiz, *Chemical Engineering Journal*, 2009, **146**, 287–294.
30 T. Yoshioka, T. Motoki and A. Okuwaki, *Industrial & engineering chemistry research*, 2001, **40**, 75–79.
31 T. Yoshioka, N. Okayama and A. Okuwaki, *Industrial & engineering chemistry research*, 1998, **37**, 336–340.
32 A. M. de Castro, A. Carniel, J. Nicomedes Junior, A. da Conceição Gomes and É. Valoni, *Journal of Industrial Microbiology and Biotechnology*, 2017, **44**, 835–844.
33 A. Göpferich, *Biomaterials*, 1996, **17**, 103–114.
34 R. Yang, M. Rodriguez-Fernandez, P. C. St. John and F. J. Doyle, in *Modelling Methodology for Physiology and Medicine (Second Edition)*, eds. E. Carson and C. Cobelli, Elsevier, Oxford, 2014, pp. 159–187.
35 G. Rahimi, S. O. Rastegar, F. R. Chianeh and T. Gu, *RSC advances*, 2020, **10**, 1685–1696.
36 B. Thangaraj and P. R. Solomon, *ChemBioEng Reviews*, 2019, **6**, 167–194.
37 T. Gitlesen, M. Bauer and P. Adlercreutz, *Biochimica et Biophysica Acta (BBA)-Lipids and Lipid Metabolism*, 1997, **1345**, 188–196.
38 O. Levenspiel, *Chemical reaction engineering*, John wiley & sons, 1998.

39 J. P. Santerre and R. S. Labow, *Journal of biomedical materials research*, 1997, **36**, 223–232.